To avoid the drift of the pure integrators in Fig. 2-23, they are often replaced by a first-order system (2.150), with a cut-off frequency f_{co} in the range of 1–4Hz.

$$\frac{1}{s} \succ \frac{1}{s + 2\pi f_{co}} \tag{2.150}$$

At frequencies higher than the cut-off frequency, the low-pass filter behaves the same as the integrator. However, at frequencies near and below the cut-off frequency, including zero frequency, the deterioration of the rotor flux estimation makes this flux observer design inoperable.

2.3.4.3 Parameter sensitivity and closed-loop flux observers

As already mentioned, the current and voltage model-based flux observers discussed in the preceding section are sensitive to errors in their parameters and in their input signals. The current model-based flux observer is primarily sensitive to the rotor resistance and the magnetizing inductance, especially when operated near to rated slip [10]. The estimation error affects both the magnitude and the phase angle of the estimated rotor flux. Conversely, the estimation of the rotor flux is insensitive to errors in the estimated leakage inductance [10]. The voltage model-based flux observer is completely insensitive to errors in the estimated rotor resistance. However, it is highly sensitive to errors in the estimated stator resistance, especially at low speeds [10]. Since the commanded voltage is normally used instead of the actual voltage, mismatch between the commanded and the actual voltage is the other relevant source of error, especially at low speeds. Careful compensation of the sources of distortion of the output voltage (inverter dead time, voltage drop in the semiconductors, etc.) is therefore needed to extend the lower frequency limit of operation of the observer [11].

Both the current and the voltage model-based rotor flux observers previously discussed are open-loop systems (i.e. do not incorporate any feedback mechanism). To improve the performance of open-loop estimators, numerous closed-loop rotor flux observers have been proposed. Frequently, these closed-loop systems estimate the stator current, the error between the estimated and the measured stator current being used to drive the rotor flux to the actual rotor flux [10].

Independent of the flux observer structure, the performance of all model-based flux observers will depend on the accuracy in the estimation of the machine parameters that they use. To guarantee adequate performance for all operating conditions, numerous methods to estimate the motor parameters can be found in the literature [12]. This can be done before the operation of the motor, as a part of the commissioning process. Such methods are normally referred to as off-line. One limitation of off-line methods is that the actual value of the motor parameters can significantly change during the normal operation of the machine. Variations of the resistance are mainly due to changes in the temperature, being therefore slow. Changes in the inductances are mainly due to saturation, and can be therefore very rapid. To compensate for these variations, several on-line estimation methods intended to estimate machine parameters dynamically and without interfering with the normal operation of the drive have been proposed [12].

2.4 Torque capability of the induction machine

The torque capability of the induction machine is limited by different factors. At low speeds, the current is limited by thermal issues. Also the rotor flux (and the other fluxes) is limited by saturation. As the speed increases, voltage limits place further restrictions, owing to the induced back-emf. At speeds above rated speed, operation at rated flux is not possible. Even if the stator current vector magnitude can still be maintained, the rotor flux needs then to be decreased. This mode of operation is referred to as field weakening.

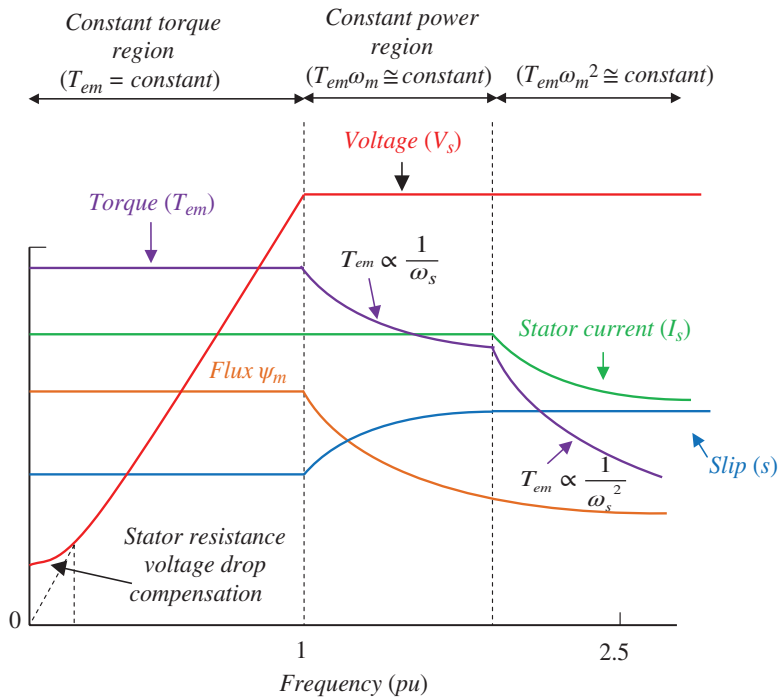

Fig. 2-24 *Operating regions of the induction machine considering voltage and current limits*

Fig. 2-24 shows the torque and rotor flux, as well as magnitude of the stator current and voltage vectors as a function of the fundamental frequency. Three different regions of operation are observed:

2.4.1 Constant torque region

- Maximum torque can be produced. Machine and power converter operate at their current limits, but below their voltage limits.
- In this mode of operation, the flux is normally kept constant and equal to its rated valued, the torque being controlled through i_{qs}.

2.4.2 Flux-weakening region I (constant power region)

- Machine and inverter reach their voltage limit. Reduction of the rotor flux is needed to operate beyond this speed. This is done by reducing the *d* axis current.
- Reduction of the rotor flux results in a decrease of the torque production capability. However, the reduction of the *d* axis current allows an increase of the *q* axis current to fully utilize the current capability of machine and inverter, partially compensating the torque reduction due to the decreased rotor flux. In this region, the machine operates therefore with reduced flux (reduced *d* axis current) but with rated voltage and current.

2.4.3 Flux-weakening region II (constant $T_{em}\omega_m^2$)

- As the speed increases, the current limit cannot be reached anymore, even if the rotor flux is reduced. Consequently, both d and q axis stator currents need to be limited. In this case, the machine operates with rated voltage but with reduced rotor flux and stator current.

The three different regions of operation are discussed in more detail in the next section.

2.5 Rotor flux selection

As already mentioned, when the machine operates below its rated speed, the rotor flux is often maintained constant and equal to its rated value. This provides excellent dynamic response, as the rotor is fully magnetized. The machine is therefore able to provide its maximum torque almost instantaneously (limited by the current control bandwidth) if required by the application. However, owing to the voltage constraints imposed by the inverter, at speeds higher than rated the rotor flux must be weakened. It is noted that this is independent of the control strategy (vector control, DTC, DSC, etc.).

Fig. 2-25 shows a generic implementation of the rotor flux reference selection block. The rotor flux limit has been shown to be a function of the machine speed. Simpler field-weakening methods therefore use the rotor speed to obtain the rotor flux command. Either the actual rotor speed or the commanded rotor speed could be used, the first option being shown in the figure. The accuracy of the rotor flux command can be enhanced if the voltage limits are taken into consideration (i.e. at high speeds the rotor flux command can be dynamically adapted to fully utilize the voltage available from the inverter, which depends on the DC bus voltage V_{bus}). In this case the inputs to the field-weakening block can be augmented with the stator voltage command and the stator voltage limit, $V_{s\ limit}$. This is schematically indicated by the dashed arrows in Fig. 2-25.

Strategies for the selection of the rotor flux are described in the following subsections.

2.5.1 Rotor flux reference selection below rated speed

It has already been shown that the rotor flux can be precisely controlled by means of the d axis current in the rotor flux reference frame. Some considerations can be made regarding the selection of the rotor flux reference.

Below rated speed, the rotor flux reference is often maintained constant and equal to its rated value. By doing this, the torque produced by the machine is only a function of the q axis current, which can be changed very quickly thanks to the high-bandwidth current regulator. This strategy therefore provides excellent dynamic response. At rated speed, the voltage limit is reached, the control entering in the field-weakening region. In this region, the flux reference decreases with the speed, to match the back-emf with the available voltage. This enables the operation at speed higher than rated, but with a reduction of the maximum torque available.

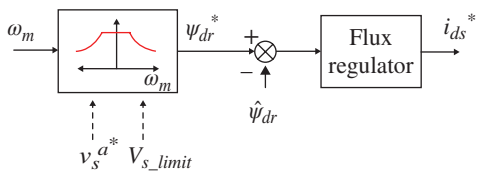

Fig. 2-25 *Rotor flux reference generation and the subsequent rotor flux regulator*

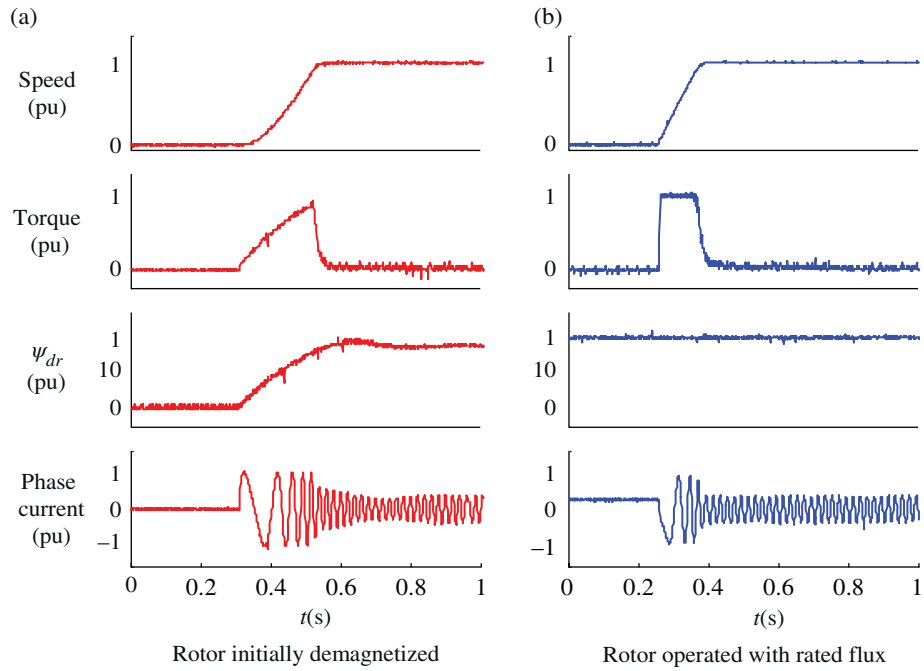

Fig. 2-26 *Dynamic response of a vector controlled induction machine during a start-up process from zero to rated speed, for the case of (a) rotor initially demagnetized and (b) rotor flux maintained equal to its rated value*

Although maintaining the rotor flux equal to its rated value at low speeds is adequate to be able to obtain good dynamic response, this is at the price of increased losses when the machine operates with light loads for long periods, as the rotor is unnecessarily magnetized in this case.

Alternatively, the machine can be operated with reduced rotor flux even below rated speed, if it is not fully loaded. With this strategy, the stator losses can be decreased thanks to the reduction of the d axis current. The reduction of the rotor flux (and of the d axis current) needs to be compensated for by an increase of the q axis current to maintain the produced torque constant, whilst the magnitude of the stator current vector is reduced. However, this reduction is at the price of a reduction of the torque dynamic response. Effectively, if the machine operates with reduced flux and the torque needs to be increased, the rotor must first be energized. The dynamics of this process are controlled by the rotor time constant, as shown by (2.135), which are significantly slower than those of the stator current control loop.

Fig. 2-26 shows the acceleration process of a speed controlled induction machine from zero to its rated speed, using the two strategies already mentioned. In the case shown in the Fig. 2-26(a), the rotor flux is initially equal to zero. It is noted that the phase current is therefore zero too; consequently, no losses exist when the machine does not produce torque. When a speed step is commanded, the rotor flux needs to be built up, the d axis current being used for this purpose (not shown in the figure). The slow dynamics building the rotor flux up results in a poor dynamic response in the torque produced by the machine, even though the q axis current was produced in the range of ms (not shown in the figure). This eventually affects to the dynamic response of the speed control loop, increasing the settling time. Conversely, in the case shown in Fig. 2-26(b), the rotor flux is maintained at its rated value. This results in losses even when the machine is not producing torque. However, when the speed step is commanded, the torque is seen to build up in a few ms (torque shown in the figure mirrors the q axis current), therefore enabling a faster response of the speed control loop.

2.5.2 Accurate criteria for flux reference generation

The method for flux reference generation explained in this section can be found in [1]. It is reproduced here for convenience, owing to its wide acceptance among electric drive designers.

First of all, the voltage and current constraints must be taken into consideration. The voltage constraints depend on the converter and the modulation. The maximum voltage provided by the converter when it operates in the linear region, and therefore the maximum available voltage that can be applied to the stator windings, is given by (2.153).

$$V_{s\_limit} = \frac{V_{bus}}{\sqrt{3}}\eta \tag{2.151}$$

It is assumed that PWM with triplen harmonic injection or space vector modulation (SVM) is used, with V_{bus} being the DC bus voltage of the power electronic converter, η: voltage efficiency of the converter (0.9–1), and V_{s_limit}: maximum phase voltage (peak).

Thus, the stator voltage limit is:

$$v_{ds}^2 + v_{qs}^2 = v_{\alpha s}^2 + v_{\beta s}^2 \le V_{s\_limit}^2 \tag{2.152}$$

On the other hand, the d–q axis stator current should comply with the current limit, I_{s_limit}, which is usually established by the thermal limit of the inverter or the AC machine itself.

$$i_{ds}^2 + i_{qs}^2 = i_{\alpha s}^2 + i_{\beta s}^2 \le I_{s\_limit}^2 \tag{2.153}$$

Performing the study at a synchronously rotating reference frame, the stator voltage can be modeled by means of the previously obtained equations (rotor flux orientation):

$$v_{ds} = R_s i_{ds} + \sigma L_s \frac{di_{ds}}{dt} - \omega_s \sigma L_s i_{qs} + \frac{L_m}{L_r}\frac{d\psi_{dr}}{dt} \tag{2.154}$$

$$v_{qs} = R_s i_{qs} + \sigma L_s \frac{di_{qs}}{dt} + \omega_s \sigma L_s i_{ds} + \omega_s \frac{L_m}{L_r}\psi_{dr} \tag{2.155}$$

Assuming steady-state conditions and neglecting the voltage drop in the stator resistances, these equations are simplified to:

$$v_{ds} \cong -\omega_s \sigma L_s i_{qs} \tag{2.156}$$

$$v_{qs} \cong \omega_s \sigma L_s i_{ds} + \omega_s \frac{L_m}{L_r}\psi_{dr} \tag{2.157}$$

Again, emphasizing that we are only considering the steady-state operation of the machine, the rotor flux is equal to:

$$\psi_{dr} = L_m i_{ds} \tag{2.158}$$

Resulting in a more compact and simplified q voltage component:

$$v_{qs} \cong \omega_s L_s i_{ds} \tag{2.159}$$

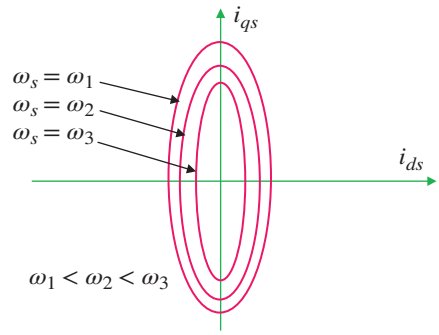

Fig. 2-27 *Ellipses at different* ω_s *due to the voltage constraint*

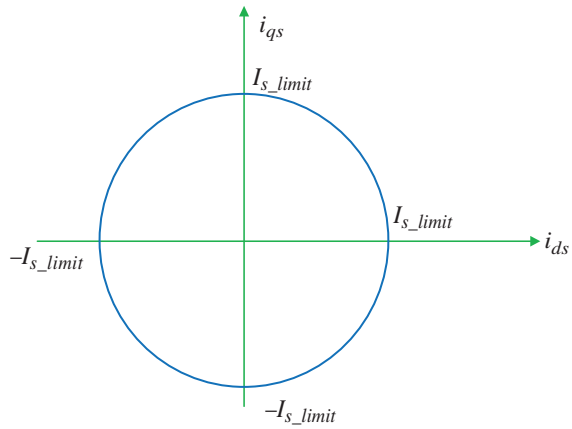

Fig. 2-28 *Circle due to the current limit*

With these simplified voltage equations in steady state, it is possible to calculate the module of the stator voltage by substituting (2.156) and (2.159) in (2.152):

$$\left(\omega_s \sigma L_s i_{qs}\right)^2 + \left(\omega_s L_s i_{ds}\right)^2 \le V_{s\_limit}^2 \tag{2.160}$$

This inequality corresponds to the area enclosed by an ellipse in the i_{ds}, i_{qs} plane, as illustrated in Fig. 2-27. Thus, the bigger ω_s it is, the smaller becomes the area of the ellipse.

On the other hand, the current constraint in the i_{ds}, i_{qs} plane corresponds to a circle, also depicted as in Fig. 2-28.

The torque can be represented as a function of the d and q axis stator currents in a rotor flux reference frame:

$$T_{em} = \frac{3}{2} p \frac{L_m^2}{L_r} i_{ds} i_{qs} \tag{2.161}$$

Constant torque values in the i_{ds}, i_{qs} plane follow the trajectory of a hyperbola, as illustrated in Fig. 2-29.

The feasible operating region (the shaded area) corresponds to the cross-section between the ellipse and the circle. Thus, in this presented example of Fig. 2-29, if the torque curve represents the maximum torque value,

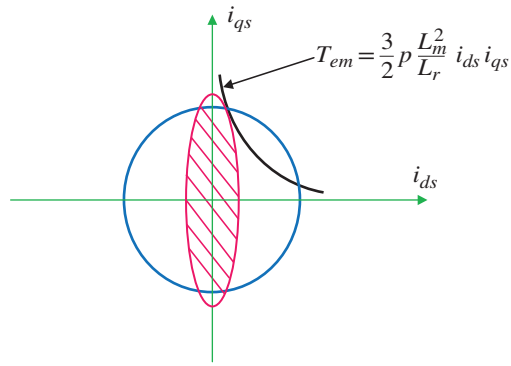

Fig. 2-29 *Constant torque characteristic, voltage, and current constraints and the permitted operation region (shaded area)*

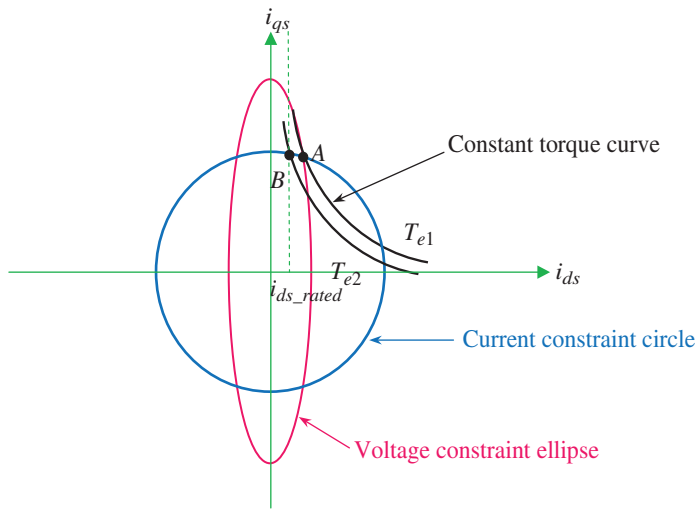

Fig. 2-30 *Voltage and current constraints and the limitation of the rated* i_{ds} *value*

only one point can satisfy the voltage and current limits. However, this point must be checked with the data given by the manufacturer of the machine. If the rated flux (rated i_{ds} because $\psi_{dr} = \psi_{dr\_rated} = L_m i_{ds} = L_m i_{ds\_rated}$) corresponds to a value smaller than the corresponding value at point A in Fig. 2-30, the maximum available torque of this machine will be the hyperbola which crosses point B in Fig. 2-30. Note that going above the rated i_{ds} value means excessively saturating the machine, increasing the losses, and deteriorating the ideal performance of the machine in general. Consequently, during constant torque region, the i_{ds} value is kept constant to:

$$i_{ds} = i_{ds\_rated} \tag{2.162}$$

while the maximum available i_{qs} value is:

$$i_{qs} = \sqrt{I_{s\_limit}^2 - i_{ds\_rated}^2} \tag{2.163}$$

The angular frequency where the constant torque operation region ends ω_b is defined as the base frequency and can be calculated according to the following formula [1]:

$$\omega_b = \sqrt{\frac{(V_{s\_limit})^2}{\psi_{dr\_rated}{}^2 \frac{L_s^2 - (\sigma L_s)^2}{L_m^2} + (\sigma L_s I_{s\_limit})^2}} \tag{2.164}$$

Field weakening operation can be separated in two regions. In region 1, the d axis current to maximize the torque can be derived from the crossing point of the ellipse and the circle:

$$i_{ds} = \sqrt{\frac{\left(\frac{V_{s\_limit}}{\omega_s}\right)^2 - (\sigma L_s I_{s\_limit})^2}{L_s^2 - (\sigma L_s)^2}} \tag{2.165}$$

Note that in region 1 the d axis current reference is always smaller than the rated d axis current, since the ellipse becomes smaller and smaller. This fact is graphically represented in Fig. 2-31. Note also that the torque that can be provided in this region is below the rated, owing to the voltage (ellipse) limitation. However, the maximum available current can still be reached.

Consequently, the rotor flux reference can be generated according to the following expression:

$$\psi_{dr} = L_m \sqrt{\frac{\left(\frac{V_{s\_limit}}{\omega_s}\right)^2 - (\sigma L_s I_{s\_limit})^2}{L_s^2 - (\sigma L_s)^2}} \tag{2.166}$$

while the remaining current for i_{qs} is:

$$i_{qs} = \sqrt{I_{slimit}^2 - (i_{ds})^2} \tag{2.167}$$

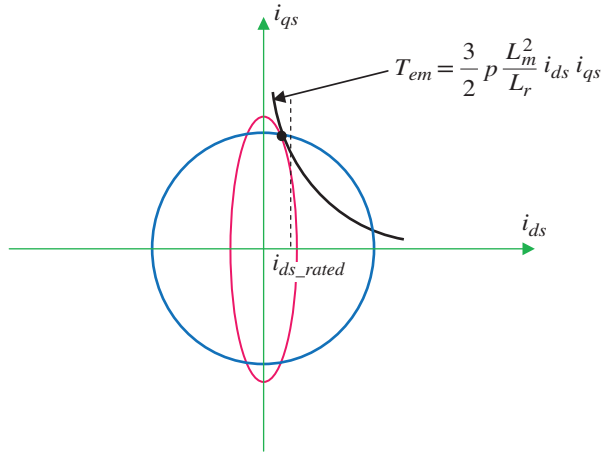

Fig. 2-31 *Voltage and current constraints in flux-weakening region 1*

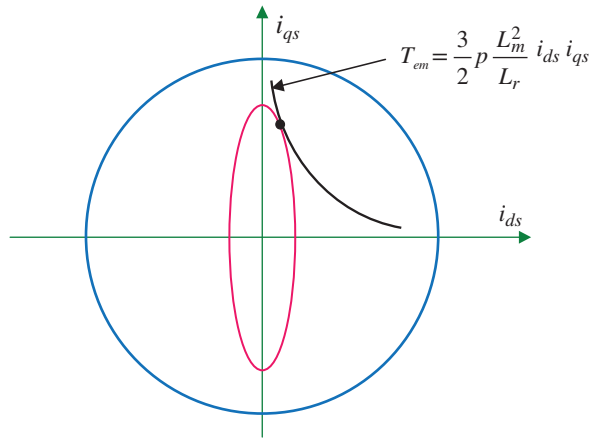

Fig. 2-32 *Voltage and current constraints in flux-weakening region 2*

Finally, if the speed further increases above a certain limit, the ellipse will be inside the circle, as depicted in Fig. 2-32. In this situation, the torque is only limited by the voltage constraint, its not being possible to reach the maximum current limit. This corresponds to region 2.

The frequency, ω_1, where the flux-weakening region 2 starts, can be derived as from the fact that at that frequency the circle meets the ellipse at a single point:

$$\omega_1 = \sqrt{\frac{L_s^2 + (\sigma L_s)^2}{2(L_s \sigma L_s)^2} \times \frac{V_{s\_limit}}{I_{s\_limit}}} \tag{2.168}$$

The reference points to maximize the torque at minimum current can be derived at the meeting points of torque and voltage curves:

$$i_{ds} = \frac{V_{slimit}}{\sqrt{2}\omega_s L_s} \tag{2.169}$$

Hence, the rotor flux reference yields:

$$\frac{\psi_{dr} = L_m V_{s\_limit}}{\sqrt{2}\omega_s L_s} \tag{2.170}$$

The q axis current can be calculated as:

$$i_{qs} = \frac{V_{s\_limit}}{\sqrt{2}\omega_s \sigma L_s} \tag{2.171}$$

As mentioned before, in this flux-weakening region 2, owing to the large values of the speed, the current limit cannot be reached because of a prevalence of the voltage limit.

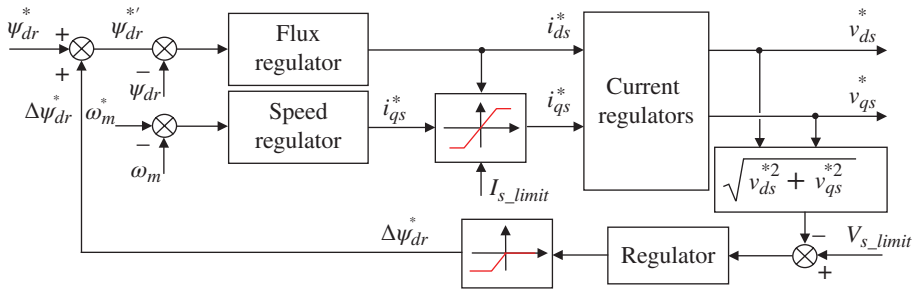

Fig. 2-33 *Flux weakening with closed-loop control*

Počasen PI regulator

2.5.3 Feedback based field weakening

Alternatively to feed-forward-based flux-weakening methods, a feedback-based strategy can be used. This method does not require the use of a machine model or pre-calculated look-up tables. Instead, the voltage command provided by the current regulator is used to dynamically adapt the flux reference to the machine speed. As illustrated in Fig. 2-33, the input to the flux-weakening regulator is the difference between the output voltage of the current regulator and the maximum available voltage, V_{s_limit}, which depends on the DC bus voltage, V_{bus}, and the PWM strategy ((2.151)). When the machine operates at frequencies below the rated frequency, the stator voltage reference set by the current regulators in steady state will be below the voltage limit V_{s_limit}. In this case, there is no need to decrease the rotor flux level, the incremental rotor flux $\Delta\psi_{dr}$ (i.e. variation of the flux reference with respect to its rated value) commanded by the flux-weakening control loop is zero. Conversely, when the frequency of the machine is equal to or larger than the rated frequency, the magnitude of the voltage reference set by the current regulators will be larger than V_{s_limit}, meaning that there is not enough voltage available in the inverter to compensate for the back-emf. This produces a negative error, which results in a decrease of the flux reference (i.e. a negative incremental rotor flux $\Delta\psi_{dr}$). The flux-weakening control loop therefore decreases the flux level until the commanded voltage matches the available voltage V_{s_limit}. It will be noted that, since the flux weakening produces a decrease of the current i_{ds}, the limit of the torque current, i_{qs}, can be increased to operate with maximum current, I_{s_limit}. A coordinated current reference limitation is implemented for this purpose, as shown in Fig. 2-33.

Tuning the flux-weakening regulator is not straightforward. Its bandwidth should be significantly lower than the current regulator bandwidth to prevent interference. However, and because of this, in a scenario of fast speed variations, the performance of this loop may present an oscillatory behavior.

2.6 Outer control loops

Though the current regulators and flux estimation blocks are the core of vector controlled induction machine drives, many applications may require the use of outer control loops to fulfill specific application requirements. These outer control loops are typically connected in cascade with the current control loops. A general block diagram is shown in Fig. 2-34. Two outer control loops for the speed and rotor flux provide the q and d axis current commands respectively. Though not shown in the figure, a position control loop can also be included, normally in cascade with the speed control loop. PI regulators are typically used for the speed and flux control, while a P controller is used for position control.

Design and tuning of speed and rotor flux control loops are discussed in this section. Position control is not discussed further in this book, as it has limited interest for the applications considered.

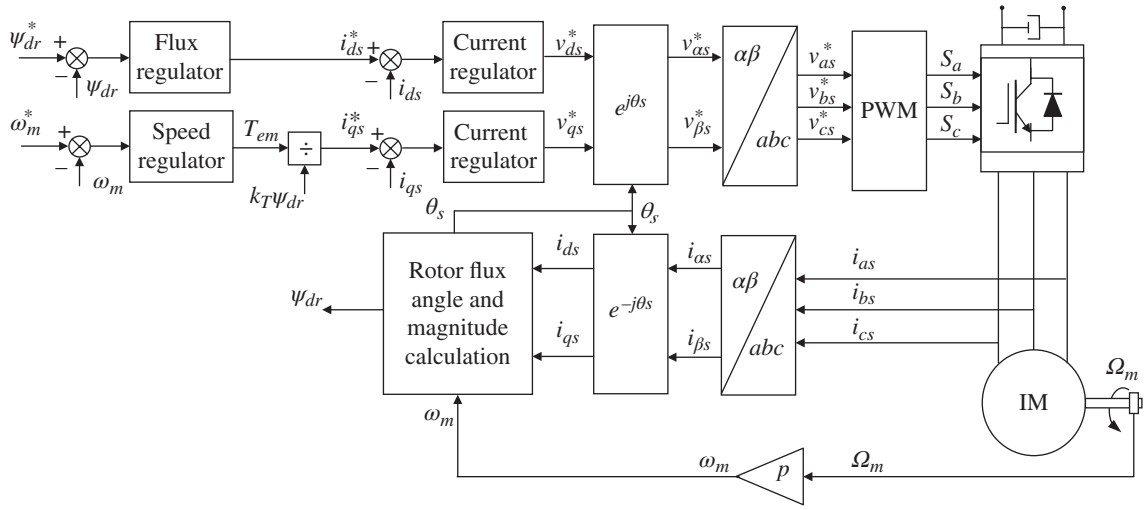

Fig. 2-34 *Field oriented control including speed and rotor flux control loops*

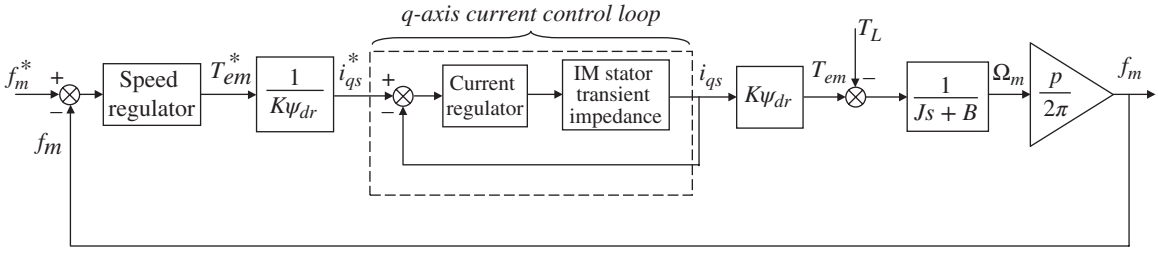

Fig. 2-35 *Simplified block diagram of the speed control loop. The controlled variable is the electrical speed in Hz* f_m, Ω_m *being the mechanical speed in rad/s*

2.6.1 Speed control

In applications requiring speed control, an outer speed control loop is added. The speed control loop provides the torque (or alternatively the q axis current) to an inner loop including current regulation and field-oriented control. This is schematically represented in Fig. 2-35. The term $1/K\psi_{dr}$ is included to make the speed-torque loop dynamics independent of the rotor flux magnitude. The speed regulator is typically PI type.

In high-performance electric drives, the current loop is tuned to have a bandwidth much faster than the speed control loop. The current control dynamics can therefore be safely neglected. Consequently, the actual torque can be assumed to be nearly equal to the commanded torque (2.172):

$$T_{em}^{*} \approx T_{em} = K\psi_{dr} i_{qs} \tag{2.172}$$

The overall mechanical equation will depend on the mechanical characteristics of the machine and load. The machine can be considered as nearly a pure mechanical, invariant inertia, friction being almost negligible. However, the mechanical characteristics of the load strongly depend on the application. Consequently,

selection of the parameters for the speed regulator will depend on the mechanical load characteristic; no general tuning procedure can be given. As an example, tuning of the speed controller for the case of a load including mechanical inertia and a viscous friction, as well as the load torque (2.173), is briefly discussed here.

$$T_{em} = T_L + J\frac{d\Omega_m}{dt} + B\Omega_m \tag{2.173}$$

The transfer function that links the electrical speed with the torque produced by the machine is:

$$\frac{f_m(s)}{T_{em}(s)} = \frac{p}{2\pi}\cdot\left(\frac{1}{Js+B}\right) \tag{2.174}$$

The dynamics of the speed control loop are normally selected to be significantly slower than those of the current control loop. This restriction comes first from the physical nature of the mechanical systems, whose time constant is significantly larger than that of the electrical subsystem. In addition, proper operation of cascaded control systems, as that shown in Fig. 2-34, requires that the inner (current) control loop behaves significantly faster than the outer (speed) control loop, as this enables independent design and tuning of both control loops.

Being the transfer function of the PI speed controller (2.175), the transfer function linking the actual speed with the speed command in electrical units is given by (2.176), while the transfer function linking the speed with the disturbance torque is (2.177).

$$PI_f = k_{pf} + \frac{k_{if}}{s}\cdot \tag{2.175}$$

$$\frac{f_m(s)}{f_m^*(s)} = \frac{k_{pf}\cdot s + k_{if}}{\frac{2\pi}{p}J\cdot s^2 + \left(\frac{2\pi}{p}B\cdot + k_{pf}\right)\cdot s + k_{if}} \tag{2.176}$$

$$\frac{f_m(s)}{T_L(s)} = \frac{s}{\frac{2\pi}{p}J\cdot s^2 + \left(\frac{2\pi}{p}B\cdot + k_{pf}\right)\cdot s + k_{if}} \tag{2.177}$$

The system dynamics are seen to correspond to those of a second-order system. Similar to that discussed for the tuning of the synchronous PI current regulator, zero-pole cancellation can be used to reduce the dynamics to those of a first-order system. To achieve this, the relationship between the mechanical parameters and the speed PI controller gains is given by (2.178). The proportional gain of the speed controller k_{pf} is then selected to achieve the desired bandwidth.

$$\frac{k_{if}}{k_{pf}} = \frac{B}{J} \tag{2.178}$$

Alternatively, the natural frequency and damping coefficient for the second order can be specified. The speed controller gains k_{pf} and k_{if} are obtained as for the current controller case, being given by (2.179)–(2.180):

$$k_{if} = \frac{2\pi J}{p}{\omega_n}^2 \tag{2.179}$$

$$k_{pf} = \frac{2\pi J}{p} 2\xi\omega_n \tag{2.180}$$

There are applications in which the mechanical friction is negligible compared to the mechanical inertia, the mechanical transfer function being in this case (2.181).

$$\frac{f_m(s)}{T_{em}(s)} = \frac{p}{2\pi} \cdot \frac{1}{Js} \tag{2.181}$$

These types of systems are often prone to show oscillatory behavior, owing to the double integrator in the closed-loop system, coming from the mechanical load and from the PI speed regulator respectively. Zero-pole cancellation cannot be used in this case, as the load pole is located at the origin. A fictitious friction can be used in this case, which is often called active damping. This is schematically shown in Fig. 2-36.

When seen from the speed regulator, the fictitious friction B' is connected in parallel with the actual friction B (if this exists), meaning that B' can be used to adjust the overall friction to the desired value. Some consideration needs to be made in this regard:

- It is noted that B' physically does not consume torque (or power). This means that the torque commanded by the speed regulator $T_{em}^{*'}$ can be larger than the maximum torque that can be provided by the machine. Of course, the torque command once the torque consumed by the fictitious friction is subtracted, T_{em}^{*} has to be limited to the maximum torque that can be provided by the machine. This needs to be taken into account when implementing the torque limitation at the speed regulator output.
- It is observed from Fig. 2-36 that when seen from the speed regulator the fictitious friction B' is connected in parallel to the actual friction. However, when seen from the load torque, B' is in the feedback path, being connected in parallel with k_{pf}. Consequently, actual and fictitious frictions have different behaviors regarding load disturbance rejection.
- The fictitious damping acts through the q axis current control loop, contrary to the actual friction, which is mechanically coupled. Therefore, in order for the fictitious damping to be effective, the dynamic response or the q axis current regulator has to be much faster than the speed control loop dynamics. It should be noted, however, that this assumption is realistic in drives using high bandwidth current regulators.

It should be added that a large number of design and tuning methodologies for speed controllers have been proposed to improve command tracking and disturbance rejection capabilities, including predictive control, sliding mode control, robust control, neural networks, and so on. Further improvements—like feedforward and load torque observers—can also be used. If the mechanical characteristics of the load can change

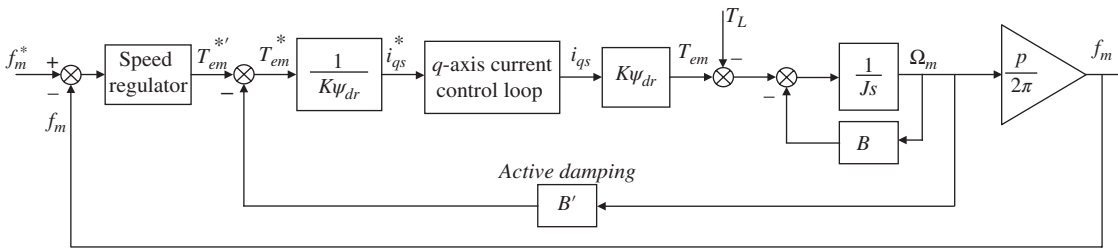

Fig. 2-36 *Speed control including active damping*

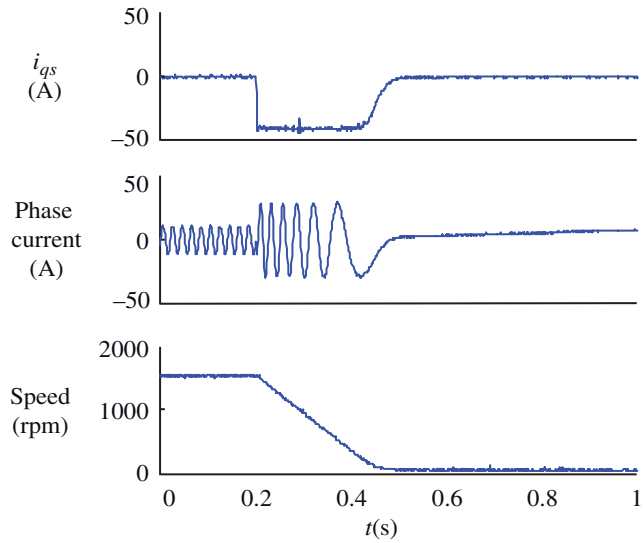

Fig. 2-37 *Dynamic response of the speed control loop*

significantly during the normal operation of the drive, the speed regulator might need to be adaptive to guarantee adequate performance under all operating conditions. On-line estimation of the load parameters is needed in this case.

Fig. 2-37 shows the typical response of the speed control loop of a vector controlled drive during a breaking process from the rated speed (1500rpm) to 0.5rpm. It is observed that for most of the transient the q axis current is saturated at its rated value. This minimizes the settling time, the resulting transient of the speed being characterized by a constant acceleration for the case of inertial loads. It can also be observed in Fig. 2-37 that if correctly tuned the speed control loop combines a fast transient with a perfectly damped response.

2.6.2 Rotor flux control loop

When a rotor flux control loop is to be implemented, the block diagram in Fig. 2-38(a) can be used. It is assumed that the rotor flux is measured. However, and contrary to the current and speed control loops, the rotor flux is never measured in practice but only ever estimated. This means that the accuracy of the rotor flux control is subject to the accuracy of the rotor flux observer. The block diagram in Fig. 2-38(b) shows the implementation of rotor flux control when the rotor flux is estimated using a current model. Obviously, the performance of the rotor flux control loop will be conditioned by the accuracy of the rotor flux observer.

For the tuning of the rotor flux regulator, it is safe to assume that the current loop bandwidth is tuned to be much faster than the rotor flux loop (as done before for the speed control loop). The dynamics of the current control loop can therefore be safely neglected. With this assumption, the equation linking the d axis current and the rotor flux is (2.182). Assuming a PI regulator with gains $k_{p\psi}$ and $k_{i\psi}$ is used, the closed-loop transfer function of the rotor flux control loop (2.183) is obtained. It should be noted that perfect rotor flux estimation has been assumed.

$$\frac{\psi_{dr}}{i_{ds}} = \frac{L_m}{\tau_r s + 1}. \tag{2.182}$$

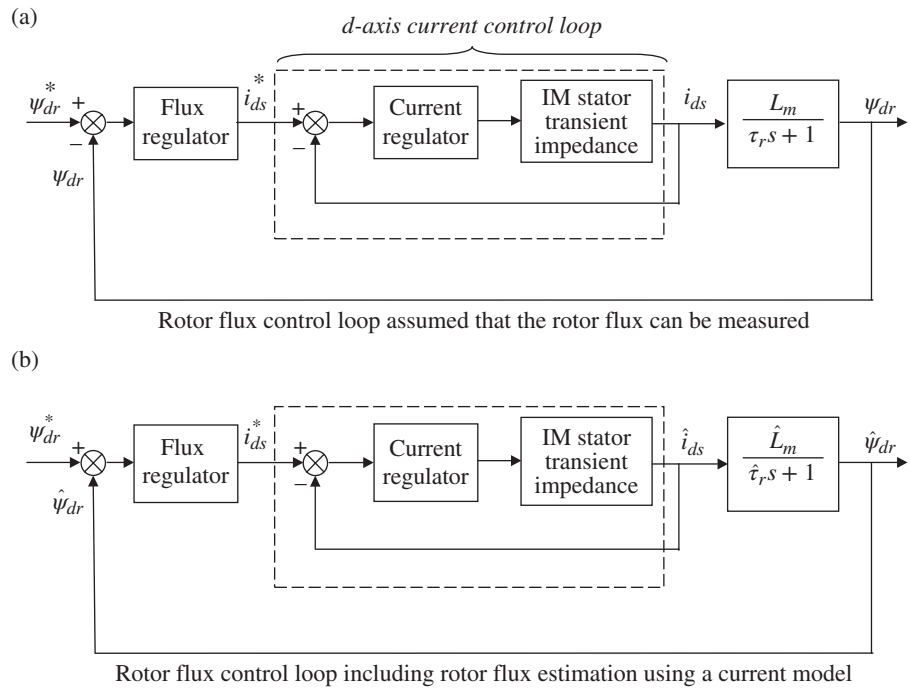

Fig. 2-38 *Ideal and actual rotor flux control loops*

$$\frac{\psi_{dr}}{\psi_{dr}{}^*} = \frac{k_{p\psi} s + k_{i\psi}}{s^2 \frac{\tau_r}{L_m} + s\left(\frac{1}{L_m} + k_{p\psi}\right) + k_{i\psi}} \tag{2.183}$$

It is observed from (2.183) that the dynamics of the rotor flux control loops corresponds to a second-order system. Therefore, the same methodology described for the current and speed control loops can be used for the rotor flux control loop. The controller gains can be selected to realize zero-pole cancellation (2.184), the resulting closed system being now reduced to a first-order system, its bandwidth being given by the selection of $k_{p\psi}$.

$$\frac{k_{i\psi}}{k_{p\psi}} = \frac{1}{\tau_r} \tag{2.184}$$

Alternatively, the gains can be selected to obtain the desired response for the second-order system in (2.183). Being ω_n and ξ, the desired natural frequency and damping factor of the closed-loop system, the rotor flux controller gains would be obtained as (2.185) and (2.186) respectively.

$$k_{i\psi} = \frac{\tau_r}{L_m} \omega_n{}^2 \tag{2.185}$$

$$k_{p\psi} = \frac{\tau_r}{L_m} 2\xi\omega_n - \frac{1}{L_m} \tag{2.186}$$